

## ASSESSMENT OF RELIABILITY OF MULTI-BEAM ECHO-SOUNDER BATHYMETRIC UNCERTAINTY PREDICTION MODELS

Tannaz H. Mohammadloo<sup>a</sup>, Mirjam Snellen<sup>a</sup>, Alireza Amiri-Simkooei<sup>a</sup>, Dick G. Simons<sup>a</sup>

<sup>a</sup>Acoustics Group, ANCE, Department of Control & Operations, Faculty of Aerospace Engineering, Delft University of Technology, Kluyverweg 1, 2629 HS, Delft, The Netherlands

Tannaz H. Mohammadloo, Kluyverweg 1, 2629 HS, Delft, The Netherlands, 0031 15 2787399, [T.Hajimohammadloo@tudelft.nl](mailto:T.Hajimohammadloo@tudelft.nl)

**Abstract:** Nowadays Multi-Beam Echo-Sounder (MBES) systems are used for obtaining information of the sea/river bed bathymetry and sediment composition. For the latter, use is usually made of the backscatter strength and depth derivatives, such as depth residuals. However, the depth derivatives are affected by the uncertainties inherent to the MBES varying with the sensors used, survey configuration and operational environment. Although models are available for the vertical uncertainty prediction, the question is how well these models can capture the estimated uncertainties of real observations. The present contribution addresses this issue by comparing the measured with modelled depth uncertainty accounting for the most recent insights of the error contributors. Data was acquired in water depths of around 2m, 10m and 30m with pulse lengths of 27  $\mu$ s, 54  $\mu$ s and 134  $\mu$ s in the Oosterschelde estuary, the Netherlands, enabling the assessment of depth and pulse length dependence of the uncertainties. In general, the predicted and measured uncertainties are in the same order of magnitude. With increasing depth the discrepancy between the modelled and measured uncertainties increases. The effect of changing pulse length is found to be captured by the model, except for the angles close to nadir. The most dominant contributors to the vertical uncertainty are those induced by the angle of impact and range measurements. These contributors thus require further investigation to obtain a more realistic estimate of the vertical uncertainties.

**Keywords:** Multibeam Echosounder Derived Depth, Bathymetric Uncertainty Prediction, Inherent MBES Uncertainty Sources

## 1. INTRODUCTION

Multibeam echosounders (MBESs) have become the most valuable tool for seafloor mapping providing a good coverage and high resolution bathymetry and acoustic backscatter datasets within a relatively short time [1]. The applications of these datasets are numerous, including offshore activities such as building wind farms at sea, the support of dredging operations, safe navigation, and the study of marine geological and biological systems [2], [3], [4], [5]. The MBES measurements used for obtaining such information are backscatter strength and depth derivatives, such as depth residuals. However, similar to any type of measured quantity, they are contaminated by uncertainties.

Obtaining a realistic a priori estimate of depth uncertainties is thus of importance as lacking information can lead to mistakenly classifying the uncertainties and assigning different sediment types to measurement having actually the same sediment composition, but different uncertainties. The realistic uncertainty description is also used for survey planning to assess whether the required survey standards can be met in a specific measurements campaign. Other applications of a-priori estimates of the vertical uncertainty include, but are not limited to, bathymetric gridding, [6], used for coastal inundation modelling, [7]. Efforts have been thus put forward to predict the depth uncertainties [8], [7], [9] and [10]. However, considering the fast development of MBES systems, there is a need to investigate the reliability of MBES depth uncertainty prediction models using real measurements to obtain an insight into their agreements and possible discrepancies and to highlight direction for future improvements.

The present contribution makes the first steps toward such a comparison and it is organized as the following. Section 2 gives a short description of the equations used for quantifying the depth uncertainties followed by the result in Section 3. The conclusions are given in Section 4.

## 2. DESCRIPTION OF THE DEPTH UNCERTAINTY PREDICTION MODEL

In an MBES system the depth of an underlying surface is determined using the travel time of a transmitted signal. A wide bundle of sound is transmitted perpendicular to the direction of vessel movement. Using electronic beam-steering at reception, the MBES can distinguish between incoming angles of sound on the transducer, [11]. The steering angle is noted by  $\theta_s$  and the resulting beams have opening angles  $\psi_y$  and  $\psi_x$  in the across-track and along-track directions respectively. The depth below the transducer,  $d$ , is determined as

$$d = r \cos P \cos(\theta_s + R + \theta_{\text{mount}}) = r \cos P \cos \theta \quad (1)$$

with  $\theta_{\text{mount}}$ ,  $R$  and  $P$  being the across track angle under which the MBES is mounted on the vessel, roll and pitch angle, respectively. Three angles represent rotations around the depth-axis and can be combined in a single rotation  $\theta = \theta_s + R + \theta_{\text{mount}}$ . Uncertainty with regard to the exact values of the parameters used for depth calculation induces a depth uncertainty. Here, a short description of the contributions is given (an interested reader might refer to [8] for a complete derivation of all equations).

- I. **Echo-Sounder contribution** which can be divided into range and angular errors. The former is induced by uncertainties in the measured travel time of the signal and speed

of sound. The across-track angular error is due to the uncertainty in the measurement of the angle of impact of the incoming sound wave at the transducer array. The combined uncertainty,  $\sigma_{EchSou}^2$ , reads as

$$\sigma_{EchSou}^2 = (\cos P \cos \theta)^2 \left[ \sigma_{r_{meas}}^2 + \left( \frac{r_{meas}}{v_{meas}} \right)^2 \sigma_{v_{meas}}^2 \right] + (r \sin \theta \cos P)^2 \sigma_{\theta_{meas}}^2 \quad (2)$$

where  $\sigma_{r_{meas}}^2$  is the error in the measured distance ( $r_{meas}$ ). It depends on the range sampling resolution and pulse length. Equation (2) is valid under the assumption that the true sound speed in the water ( $v$ ) does not deviate too much from the measured average sound speed in the water column ( $v_{meas}$ ).  $\sigma_{\theta_{meas}}^2$  is the random error in the measurements of the impact angle and depends on the measurement method (phase or amplitude detection), as

$$\sigma_{\theta_{meas}} = \begin{cases} \frac{\psi_y}{12} & \text{Amplitude detection} \\ \frac{0.2\psi_y}{\sqrt{n_p}} & \text{Phase detection} \end{cases} \quad (3)$$

with  $n_p$  the number of phase samples, defined as  $(\frac{d\psi_y}{\cos^2 \theta}) / (\frac{\tau v}{2 \sin \theta})$  where  $\tau$  indicates the pulse length. In Ref. [8], it is indicated that the phase detection is applied for situations in which  $n_p > 12$ . For the present contribution, the detection type is chosen automatically based on the minimum of angular measurements errors induced by the amplitude and phase detection. Equation (3) does not take the impact of a particular pulse shape into account. An alternative approach presented in [9] does account for the uncertainties in the detection instant in the interferometry step using the coherence coefficient which is a measure for the correlation between the two received signals at the two sub-arrays. In this case the pulse shape is taken into account.

**II. Angular Motion Sensor contribution** due to the uncertainty in the measurement of roll and pitch denoted by  $\sigma_{R_{meas}}^2$  and  $\sigma_{P_{meas}}^2$ , respectively. The resulting random depth error reads as

$$\sigma_{Ang\_Mot}^2 = (r \cos P \sin \theta)^2 \sigma_{R_{meas}}^2 + (r \cos \theta \sin P)^2 \sigma_{P_{meas}}^2 \quad (4)$$

In case of applying roll and pitch corrections during beamforming, a second pair of roll and pitch errors are added due to account for the errors made by this stabilization.

**III. Motion Sensor/Transducer Alignment contribution** due to incorrect alignment of the motion sensor, i.e., roll ( $\Delta R_{Align}$ ) and pitch ( $\Delta P_{Align}$ ), with the MBES transducer and induces a depth uncertainty as

$$\sigma_{MotSen\_Align}^2 = (r \cos P \sin \theta)^2 \sigma_{\Delta R_{Align}}^2 + (r \cos \theta \sin P)^2 \sigma_{\Delta P_{Align}}^2 \quad (5)$$

where the first and second terms in Eq. (5) indicate the contribution of roll and pitch incorrect alignment, respectively. Again, if mechanical pitch and roll stabilization is active, a second pair of  $\sigma_{\Delta R_{align}}^2$  and  $\sigma_{\Delta P_{align}}^2$  is added to Eq. (5).

- IV. Sound Speed contribution** due to errors in the sound speed at the transducer,  $\sigma_{v,s}^2$ , and that of the water column,  $\sigma_{v,p}^2$ . These uncertainties induce uncertainty in the steering angle and consequently the measured depth. The contribution reads as

$$\sigma_{\text{SoundSpeed}}^2 = (r \cos P \sin \theta)^2 \left[ \left( \frac{\tan \theta_s}{v_s} \right)^2 \sigma_{v,s}^2 + \left( \frac{\tan \theta}{2v_p} \right)^2 \sigma_{v,p}^2 \right] \quad (6)$$

where the first term in brackets in Eq. (6) represents errors in the beam steering angle due to fluctuations of the sound speed at the transducer and depends on the angle relative to the normal of the transducer,  $\theta_s$ , and  $v_s$  is the surface sound speed. The second term in bracket in Eq. (6) is the contribution of the non-uniform sound speed profile to the random depth error. Varying sound speed in the water column result in the deviation of the sound waves from straight lines. This is accounted for in the MBES processing but uncertainties in the water column sound speed profile measurements induce errors in the resulting bathymetry. The above expression for the quantification of this errors source is based on the assumption a two-layer sound speed profile.

- V. Heave contribution** due to measurements error of heave and roll and pitch errors. The depth uncertainty due to the heave contribution reads as

$$\sigma_H^2 = \max(a^2, (bH_{\text{meas}})^2) + \sigma_{H_{\text{Induced}}}^2 \quad (7)$$

where the first term in Eq. (7) represents the uncertainty in the heave measurements with  $a$  being a static component in meters and  $b$  a variable component. In case of using the Global Navigation Satellite System (GNSS) sensor for heave measurements, the first term is substituted with the uncertainty of the sensor's  $z$ -component. Heave induced uncertainty is due to the errors in the roll and pitch measurements, their alignment and the fact that the vertical reference unit, VRU, (or GNSS sensor in case of using it for heave determination) is not located at the same position as the transducer resulting in a deviation between the measured heave and the heave at the transducer. The corresponding induced depth uncertainty reads as

$$\begin{aligned} \sigma_{H_{\text{Induced}}}^2 = & (x \cos P - y \sin R \sin P - z \cos R \sin P)^2 \left( \sigma_{P_{\text{meas}}}^2 + \sigma_{\Delta P_{\text{Align}}}^2 \right) \\ & + (y \cos R \cos P - z \sin R \cos P)^2 \left( \sigma_{R_{\text{meas}}}^2 + \sigma_{\Delta R_{\text{Align}}}^2 \right) \\ & + \sin^2 P \sigma_x^2 + \sin^2 R \cos^2 P \sigma_y^2 + (1 - \cos R \cos P)^2 \sigma_z^2 \end{aligned} \quad (8)$$

where  $x$ ,  $y$ , and  $z$  are the offset coordinates between the transducer and VRU. Here,  $\sigma_x^2$ ,  $\sigma_y^2$  and  $\sigma_z^2$  are the errors in the measurement of the distance between the VRU and MBES. In case the vertical positioning is carried out using the GNSS and the position corrections are received from Real Time Kinematic (RTK) services, the depth relative to the vertical datum is derived and accounting for height offset, such as dynamic

draft and tidal variations, in not of importance. Otherwise, a separate contribution will be added, see [8].

Assuming the above contributors are uncorrelated, the total depth error is calculated as

$$\sigma_d^2 = \sqrt{\sigma_{EchSou}^2 + \sigma_{Ang\_Mot}^2 + \sigma_{MotSen\_Align}^2 + \sigma_{SoundSpeed}^2 + \sigma_H^2} \quad (9)$$

### 3. RESULTS

This section focuses on quantifying the predicted depth uncertainties for different environmental conditions and operation setting. The predictions are derived for a situation where the EM2040c MBES (manufactured by Kongsberg) is used, and its characteristic are thus used as the input parameters, see [12]. In addition to the MBES characteristics, information regarding the uncertainties of the sound speed measurements and motion sensors are of importance. For this study a case is considered where the inertial navigation sensor and sound velocity profiler used are Phins (manufactured by iXblue) with nominal roll and pitch accuracies equalling  $0.01^\circ$  and miniSVP (manufactured by Valeport) with a nominal accuracy of  $0.02\text{m/s}$ , respectively, see [13] and [14]. However, from measurements in different locations (inland waterways and the North Sea), the uncertainty of the latter was found to be  $0.2\text{m/s}$ , and hence this value is chosen as a more realistic description of the system’s accuracy. The sound velocity profile acquired was almost constant through the water column equalling  $1515\text{m/s}$ . Shown in Fig. 1 is the total predicted vertical uncertainty as a function of depth for pulse lengths of  $27\ \mu\text{s}$ , (a), and  $134\ \mu\text{s}$ , (b) for 4 different beam angles. As seen, an increase in the pulse length deteriorates the vertical accuracy for all beam angles. For beams close to nadir, the increased uncertainty with depth (black solid line) is negligible, however, as the beam angle increases, the vertical uncertainty increases to a larger extent.

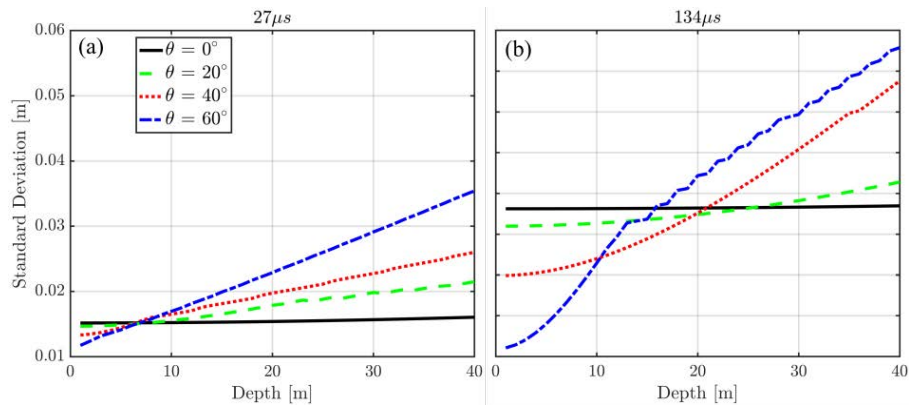


Fig. 1: Predicted depth uncertainty as a function of depth for pulse length of  $27\ \mu\text{s}$  (a) and  $134\ \mu\text{s}$  (b)

Shown in Fig. 2 is the total vertical uncertainty predicted as a function of pulse length for depths of 2 m, (a), and 30 m, (b). For the depth of 2 m and shortest pulse length, the predicted uncertainty is almost equal for all the beam angles. As the pulse length increases, the discrepancy between the predictions for varying beam angle increases with the predictions being larger at nadir. As one moves to deeper depths, (b), the behavior of the predictions changes compared to those of the shallower depth. This means that for the shortest pulse length, the uncertainty increases toward the outer parts of the swath. As seen, for the beam

away from nadir ( $20^\circ$  (green),  $40^\circ$  (red) and  $60^\circ$  (blue)) the predictions show almost equal increase in the uncertainty with the pulse length. However, this is not the case for shallower depth as the rate of the increase with the pulse length decreases towards the outer parts of the swath.

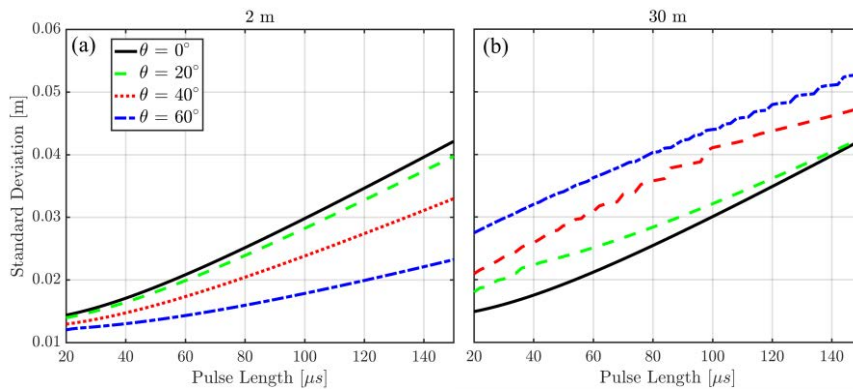


Fig. 2: Predicted depth uncertainty as a function of pulse length for water depth of 2 m (a) and 30 m (b)

The assessment of the dependency of the predicted uncertainties to depth, beam angle and pulse length indicates that varying MBES settings and operational environments can significantly affect the vertical uncertainties. Therefore, a realistic description of this parameter is needed for employing the depth derivatives, such as depth residuals ([4] and [15]), as a potential classifier in seafloor sediment classification methods. This means that for a certain MBES setting and operational environment, lacking knowledge of the vertical uncertainties can lead to interpreting the observed depth variations as varying sediment types although they might be induced by the depth uncertainty sources inherent to the MBES.

To assess the reliability of the uncertainty prediction model, the predicted depth uncertainty is compared to that measured. Shown in Fig. 3 is the measured (blue) and total (cyan) predicted vertical standard deviation in water depth of 10 m with pulse length of  $27 \mu$ s (a) and  $134 \mu$ s (b). The contribution of the individual sources is also shown. The black vertical lines indicate the beam angle where the switch from the amplitude to phase detection occurs based on the minimum standard deviation induced by both detection methods. The blue squares and asterisks represent the amplitude and phase detection based on the measurements, respectively. The theoretical beam angle corresponding to the change in the bottom detection method does not coincide with the one found for the measurements. This indicates that the criteria used for obtaining this transition point require modification possibly by accounting for the characteristics of the received signal.

As the pulse length increases, a broader range of beam angles around nadir (both based on predictions and measurements) use amplitude detection which is due to the phenomenon referred to as the baseline decorrelation. Longer pulse length means larger footprints on the seafloor, and hence a more fluctuating directivity pattern resulting in a noisy estimate of the zero-crossing of the phase difference (used for the phase detection). Therefore, amplitude detection becomes the preferred bottom detection approach. Generally, for both pulse lengths, the predicted and measured uncertainties are in the same order of magnitude with larger uncertainties for longer pulse lengths (b). For the shorter pulse length, there is a good agreement for the beams larger than  $10^\circ$  and the discrepancies occur for the beams closer to nadir. Potential improvements in the agreement can be obtained by further investigation of the term associated to the echosounder contribution (see the black circles) as 1) it is the most

dominant uncertainty source and 2) it depends on the bottom detection approach. As for the measurements with the longer pulse length, slightly better agreement between the measured and modelled uncertainties is obtained for starboard. The larger variations in depth uncertainty for the port side can be due to the existence of a strong bottom morphology. Here, the results are derived by subtracting the mean depth per small surfaces. However, for some areas, this will not fully account for the changes in the bathymetry induced due to the presence of local slopes. One approach to address this issue is to fit a bi-quadratic or linear function to the measurements located within small surfaces and calculate the standard deviation which is now under further investigation.

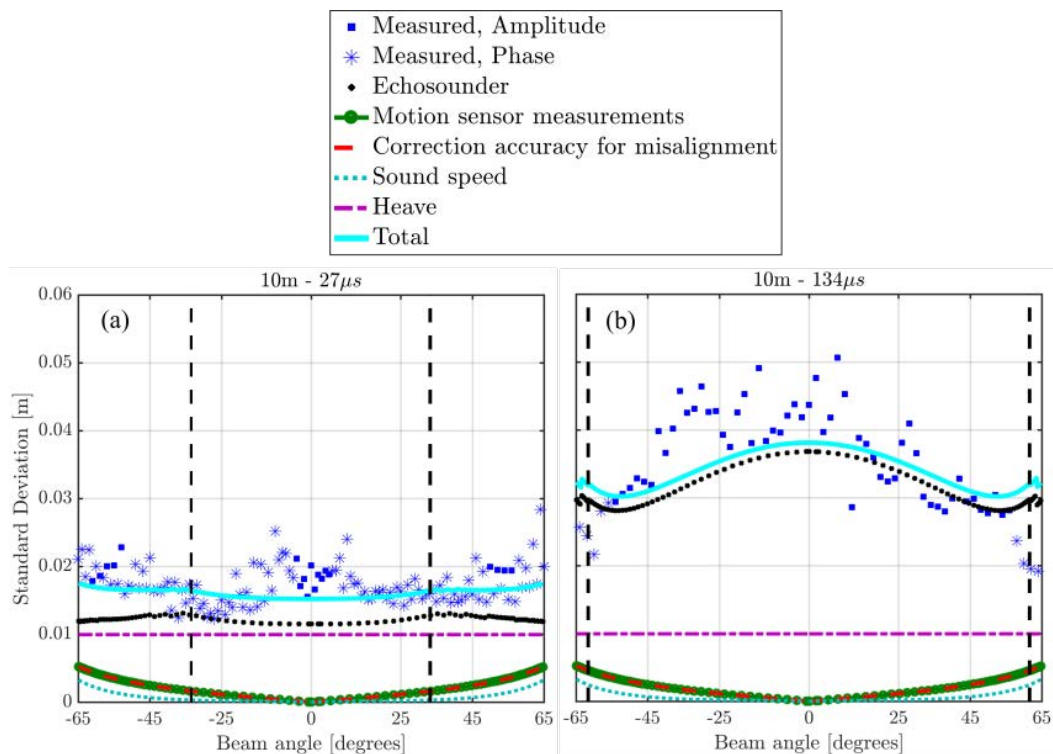


Fig. 3. Measured vertical standard deviation and those predicted for water depth of 10 m and pulse lengths of  $27 \mu\text{s}$  (a) and  $134 \mu\text{s}$  (b). The black vertical lines shows the location the beam angle where the switch from amplitude to the phase detection occurs according to the criterion of minimum standard deviation.

#### 4. CONCLUSIONS

The performance of the sediment classification approaches can be potentially improved by including the depth derivatives, such as depth residuals. However, these depth measurements are contaminated by the uncertainties in the measured depths depending on a number of parameters, such as survey configuration. A realistic description of the vertical uncertainties is thus required to ensure that the variation of the depth derivatives is due to the variation in the sediment type and not induced by the vertical uncertainties. The modelled and measured vertical standard deviation are thus compared to assess their agreement and directions for possible improvements. In general, the predicted and measured uncertainties are in the same order of magnitude. Vertical uncertainty increases with both an increasing pulse length and depth. To obtain a better agreement between the predicted and measured uncertainties, one can 1) account for the presence of local slopes as the model is developed assuming a flat

seafloor, and 2) further investigate the contribution of the echosounder as it is the most dominant error source with dependency on the detection method.

## REFERENCES

- [1] V. Lecours, M. F. J. Dolan, A. Micallef and V. L. Lucieer, "A review of marine geomorphometry, the quantitative study of the seafloor," *Hydrology and Earth System Science*, vol. 20, p. 3207–3244, 2016.
- [2] J. J. Daniell, P. T. Harris, M. G. Hughes, M. Hemer and A. Heap, "The potential impact of bedform migration on seagrass communities," *Continental Shelf Research*, vol. 28, no. 16, p. 2188–2202, 2008.
- [3] V. E. Kostylev, B. J. Todd, G. B. J. Fader, R. C. Courtney, G. D. M. Cameron and R. A. Pickrill, "Benthic habitat mapping on the Scotian Shelf based on multibeam bathymetry, surficial geology and sea floor photographs," *Marine Ecology Progress Series*, vol. 219, pp. 121-137, 2001.
- [4] D. Eleftherakis, A. R. Amiri-Simkooei, M. Snellen and D. G. Simons, "Improving riverbed sediment classification using backscatter and depth residual features of multi-beam echo-sounder systems," *J. Acoust. Soc. Am.*, vol. 131, no. 5, pp. 3710-3725, 2012.
- [5] J. E. Hughes Clarke, L. A. Mayer and D. E. Wells, "Shallow-water imaging multibeam sonars: A new tool for investigating seafloor processes in the coastal zone and on the continental shelf," *Marine Geophysical Researches*, vol. 18, no. 6, p. 607–629, 1996.
- [6] B. R. Calder and L. A. Mayer, "Automatic processing of high-rate, high-density multibeam echosounder data," *Geochem Geophys Geosyst*, vol. 4, no. 6, pp. 1048-1069, 2003.
- [7] R. Hare, B. Eakins, C. Amante and L. A. Taylor, "Modeling bathymetric uncertainty," in *US Hydro 2011*, Tampa, FL, 2011.
- [8] R. Hare, "Error Budget Analysis for US Naval Oceanographic Office (NAVOCEANO) Hydrographic Survey Systems," Hydrographic Science Research Center (HSRC), Mississippi, 2001.
- [9] T. H. Mohammadloo, M. Snellen and D. G. Simons, "Multi-beam echo-sounder bathymetric measurements: Implications of using frequency modulated pulses," *The Journal of the Acoustical Society of America*, vol. 144, no. 2, pp. 842-860, 2018.
- [10] X. Lurton and J. M. Augustin, "A measurement quality factor for swath bathymetry sounders," *IEEE J. Ocean. Eng.*, vol. 35, no. 4, pp. 852-862, 2010.
- [11] X. Lurton, *An Introduction to Underwater Acoustics, Principles and Applications*, Second edition, Springer-Verlag Berlin Heidelberg, 2010, pp. 167-224, 225-270.
- [12] Kongsberg, *EM 2040C*, Kongsberg, 2017.
- [13] *Phins: FOG-based high-performance inertial navigation system*, iXblue, March 2017.
- [14] *miniSVP - Sound Velocity Profiler*, Valeport, May 2016.
- [15] D. Eleftherakis, M. Snellen, A. Amiri-Simkooei and D. G. Simons, "Observations regarding coarse sediment classification based on multi-beam echo-sounder's backscatter strength and depth residuals in Dutch rivers," *Journal of Acoustical Society of America*, vol. 135, p. 3305, 2014.